

CLONING AND CHARACTERIZATION OF FARNESYL PYROPHOSPHATE SYNTHASE GENE FROM *ANOECTOCHILUS*

LIN YANG^{1,2}, JUN CHENG ZHANG², WAN CHEN LI¹, JING TAO QU¹, HAO QIANG YU¹,
FU XING JIANG^{3*} AND FENG LING FU^{1*}

¹Maize Research Institute, Sichuan Agricultural University, Chengdu, Sichuan 611130, PR China

²Sanming University, Sanming, Fujian 365004, People's Republic of China

³College of Landscape Architecture, Sichuan Agricultural University, Chengdu, Sichuan 611130, PR China

*Corresponding author's email: bnjfx@126.com; ffl@sicau.edu.cn

Abstract

Anoectochilus roxburghii and *Anoectochilus formosanus* are the two important species of genus *Anoectochilus* used as herbal drug and health food in traditional Chinese medicine for their abundant polysaccharides, glycoside derivative kinsenoside, and terpenoids. Farnesyl pyrophosphate synthase (FPS) catalyzes the key step of isoprenoid biosynthesis. Based on transcriptomic analysis, the open reading frame sequences of the FPS genes were obtained from *A. roxburghii* and *A. formosanus*. After bioinformatics analysis for high homology with their orthologs in related species and conserved domains of the FPS proteins, they were identified as the FPS genes of *A. roxburghii* and *A. formosanus*, respectively, and registered at GenBank. The FPS-eGFP fusion protein was specifically distributed in the cytoplasm and nucleus by transient expression in onion. Meanwhile, the expression of the FPS genes was detectable from leaf, root, and stem of these two species by real-time quantitative PCR, although their relative expression levels were significantly higher in root and stem. In response to high salt treatment, the expression of the FPS gene was downregulated in *A. roxburghii* and kept constant in *A. formosanus*. Under the illumination of red light, the downregulated range of the expression of the FPS gene in *A. roxburghii* was narrower than that in *A. formosanus*. These results suggest that *A. formosanus* has higher tolerance to salt stress, and *A. roxburghii* is more suitable for cultivation under shade environment under forest.

Key words: *Anoectochilus roxburghii*, *Anoectochilus formosanus*, Differential expression, FPS, Red light, Saline.

Introduction

Anoectochilus is a genus of family *Orchidaceae*. This genus encompasses twenty-five species, and six of them are distributed in China (Lang *et al.*, 1999). *A. roxburghii* and *A. formosanus*, native to Fujian and Taiwan provinces respectively, are the two important species used as herbal drug and health food in traditional Chinese medicine. In recent years, their wild populations are gradually depleted because of extensive collection and ecological deterioration. Artificial cultivation and tissue culture were employed to meet market demand (Shiau *et al.*, 2002; Zhang *et al.*, 2010). In most cases, the cultivation is practiced under forest for their shade-tolerant and hygrophilous properties and the consideration of filed management (Shao *et al.*, 2017). However, the accumulation of the pharmaceutical constituents in the cultivated plants is much different from the wild plants (Du *et al.*, 2000). Cultivation conditions, such as saline and light quality, affected the accumulation of the pharmaceutical constituents (Xiao *et al.*, 2014; Ye *et al.*, 2017).

Except the abundant polysaccharides for their antioxidant, hepatoprotective, antihyperglycemic, renal-protective, vascular-protective and prebiotic bioactivities (Cui *et al.*, 2013; Li *et al.*, 2016; Liu *et al.*, 2017; Yang *et al.*, 2012; Yang *et al.*, 2017; Zeng *et al.*, 2016; Zeng *et al.*, 2017; Zhang *et al.*, 2015), and glycoside derivative kinsenoside for its suppressive effects on inflammation, CCl₄-induced oxidative liver damage, umbilical vein dysfunction, as well as tumor diseases (Cheng *et al.*, 2015; Du *et al.*, 2001; Du *et al.*, 2008; Hsiao *et al.*, 2011; Hsiao *et al.*, 2016; Liu *et al.*, 2016; Shyur *et al.*, 2004; Wu *et al.*, 2007; Xiang *et al.*, 2016; Yang *et al.*, 2014; Zhang *et al.*, 2007), steroids, saponins and some other terpenoids are the other primary constituents for their suppressive effects on immune and tumor diseases (Han *et al.*, 2010; Huang *et al.*, 2015).

Terpenoids are biosynthesized from isopentenyl-5-pyrophosphate (IPP) and dimethylallyl pyrophosphate (DMPP). After the head-to-tail condensation of DMPP with two molecules of IPP to produce geranyl pyrophosphate (GPP), the transfer from GPP to farnesyl pyrophosphate (FPP) was catalyzed by FPS (Chappell, 1995; Falcone Ferreyra *et al.*, 2012). FPP is the biosynthesis precursor of sesquiterpenes, triterpenes, and steroids (Szkopinska & Płochocka, 2005). Therefore, FPS is a branch-point enzyme of terpenoid biosynthesis in plants. It also performs a regulatory function in phytosterol biosynthesis (Fig. 1) (Kim *et al.*, 2010). Therefore, cloning and characterization of the FPS genes from these two species would be helpful for further study on cultivation regulation of isoprenoid biosynthesis.

Based on the homologous amplification and rapid amplification of cDNA ends (RACE), the FPS genes have been cloned and characterized from various medicinal plants, such as *Ginkgo biloba* (Wang *et al.*, 2004), *Taxus media* (Liao *et al.*, 2006), *Panax ginseng* (Kim *et al.*, 2014), *Matricaria recutita* (Su *et al.*, 2015), *Tripterygium wilfordii* (Zhao *et al.*, 2015). However, the genomic information has not been available for homologous amplification for any species of the genus *Anoectochilus*. The differential expression of the FPS genes or activity of their encoding protein were found in response to light quality and related to terpenoid accumulation in other plants (Arena *et al.*, 2016). In the present study, the transcriptomic information were analyzed by RNA sequencing (RNA-seq) and used for homologous amplification of the potential FPS genes from *A. roxburghii* and *A. formosanus*. After sequencing and bioinformatics analysis, the subcellular localization and their expression differentiation in response to high salt treatment and the induction of red light and ultraviolet (UV) was detected.

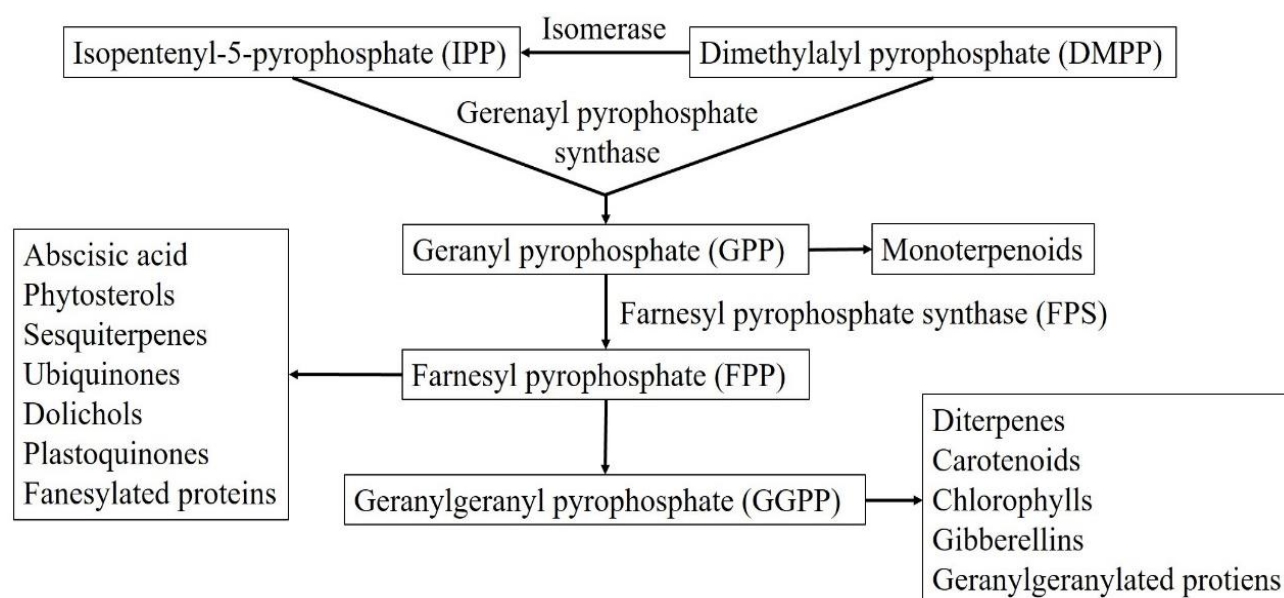


Fig.1. Terpenoid biosynthesis in plant. Farnesyl pyrophosphate synthase (FPS) catalyzes the transfer from GPP to farnesyl pyrophosphate (FPP) after the head-to tail condensation of dimethylallyl pyrophosphate (DMPP) with two molecules of isopentenyl-5-pyrophosphate (IPP) to produce GPP.

Materials and Methods

Sample preparation: The seedlings of *A. roxburghii* and *A. formosanus* were cultured on MS medium (Murashige & Skoog, 1962) for 18 weeks. Seventy-two uniform seedlings of each species were divided into three groups. One group was transplanted into a plastic box for hydroponics culture in Hoagland's solution (Hoagland & Arnon, 1950) at 28°C, relative humidity of 60%-80%, illumination of 200 $\mu\text{mol}/\text{m}^2 \text{ s}^{-1}$ (12-h light / 12-h dark) and modest aeration. On the fifth day, NaCl concentration of the nutrient solution was increased upto 100 mmol/L for high salt treatment. The other two groups were transplanted into plastic pots (three seedlings per pot) with nutritional soil and vermiculite (3:1), and grown under the illumination of 650 nm red light and 253.7 nm UV, respectively.

At 0 (control), 0.5, 1, 2, 4, 8, 12, and 24 h of the high salt and UV treatments, and 0 (control), 0.5, 1, 2, 4, 8 and 12 h of the red-light treatment, three seedlings (biological replicates) were sampled. Their leaves, roots and stems were separated and used for total RNA isolation with QiagenRNeasy plant mini kit (Qiagen, China). After release of probable DNA contamination by RNase-free DNase I (Qiagen, China), detection for purity, concentration and integrity, the RNA samples were used for reverse transcription to synthesize cDNA and kept at -20°C.

RNA-seq and transcript assembly: Part of the RNA samples of leaf and stem of the control (0 h) was mixed and sequenced by IlluminaHiSeqXten platform at MajorbioBioTech Co., Ltd. (China). The 150 bp forward and reverse raw reads were generated and deposited in FASTQ files (Cock *et al.*, 2010). The low-quality reads were filtered by using software FASTQC and NGS-QC, to release: (1) contaminated by the adaptors; (2) N (unknown base) content more than 1%; (3) base quality lower than 15 more than 50% of the reads (Patel & Jain,

2012). The clean reads were assembled by Trinity v2.4.0 (Grabherr *et al.*, 2011), clustered for unique transcripts by SWSSPROT and KOG (Feng *et al.*, 2012), and were used to query against Trans Decoderv 2.0.1 for functional annotation.

Cloning of the *FPS* gene: A pair of the *FPS* genes primers (5'-ATGGAGGAAGGGGACAGGA-3'/5'-CTAC TTTTGCCTTTTATAAATCTTATGA-3') was synthesized to amplify the ORF from the mixed cDNA samples of *A. roxburghii* and *A. formosanus* according to the annotation of RNA-seq by using primer 5.0. PCR amplification was carried out by using PrimeSTAR HS DNA Polymerase (TaKaRa, Dalian). The temperature cycle was pre-denatured at 95°C for 2 min; 38 cycles of denatured at 98°C for 30 s, annealed at 52°C for 30 s, elongated at 72°C for 90 s; and final extension at 72°C for 5 min. Using 2% agarose gel electrophoresis, the amplified products were separated, and purified by using Universal DNA Purification Kit (Tiangen, Baijing), added dATP at the tail by using *Taq*TM (TaKaRa, Dalian), subcloned into the pMD19-T vector (TaKaRa, Dalian), and sequenced at Sangon Biotech (Shanghai).

Bioinformatics analysis: The sequencing results were aligned against NCBI website, and predicted for the physical and chemical properties, secondary structure, signal peptide, and tertiary structure by using ProtParam, GOR IV, SignalP 4.1, TMHMM Server v. 2.0, and SWISS-MODEL software or databases, respectively. The subcellular localization of the putative proteins of the two amplified fragments was predicted by using the WoLF PSORT software, and presented as the nearest neighborpoints of the k-nearest neighbor algorithm (Hwang & Wen, 1998). The putative FPS proteins of *Dendrobium huoshanense* and *Cymbidium goeringii* were used as reference to improve prediction reliability. Multiple alignment among the FPS proteins from

Anoectochilus and other plants was conducted by using the online tool BLASTn software. Phylogenetic analysis was made among the putative proteins of the two amplified fragments and the deposited full-length cDNA sequences at the NCBI database with the method of maximum likelihood of 1000 bootstrap replicates by using MEGA7.0 software. The evolutionary distances were computed by using the Poisson correction method.

Subcellular localization: The *FPS* gene was amplified from the subcloned pMD19-T vector without the stop codon (TAG), using the primers (5'-catttgagagg acaggg taccggg ATGGAGGAAGGGGACAGGA-3'/5'-tcgccct gtcaccatgttactagt CTTTTCCTTTTATAAATCTTAT GA-3' with the restriction sites of *Sma*I and *Spe*I (underlined). The bases in lowercase letters were homologous to the polyclonal sites of the pC2300-*eGFP* vector, which contained an in-frame fusion gene *FPS-eGFP* under the control of constitutive promoter *CaMV 35S* and the terminator *OCS* (Fig. S.1). After identification by bacterial sequencing at Sangon Biotech (Shanghai), the recombinated vector pC2300-35S-*FPS-eGFP* (the control vector pC2300-35S-*eGFP*) was transformed into the inner epidermis of onion (*Allium cepa*). The green fluorescence signal was detected on microscope Olympus BX63 (Yu *et al.*, 2018).

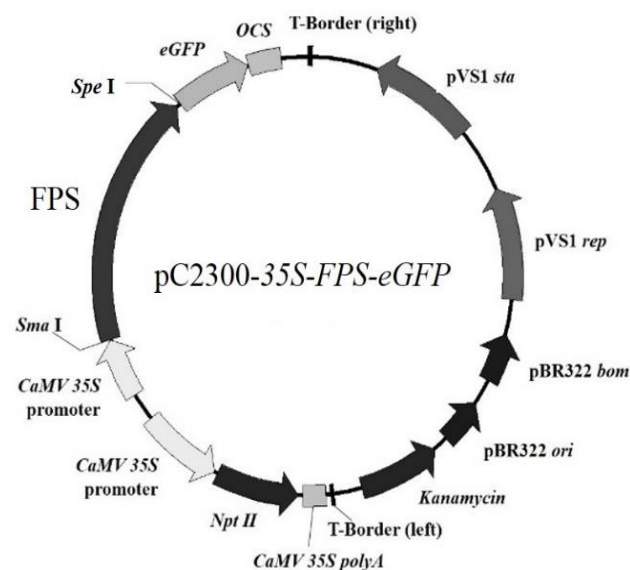


Fig. S.1. Transient expression vector pC2300-35S-*FPS-eGFP*.

RT-qPCR: For RT-qPCR detection, a pair of the *FPS* gene primers (5'-AGGTGGGAAGCTCAATCGTG-3'/5'-GCCTAGTGTGGGAGTTGTCC-3') was synthesized to amplify a 173 bp fragment in *A. roxburghii* and *A. formosanus*. Another pair of *Actin2* gene primers (5'-CGGGCATTACGAGACCAC-3'/ 5'-AATAGACCTC CAATCCAGACACT-3') was synthesized to amplify a 221 bp fragment and used as internal control (Zhang *et al.*, 2012). Using Sso Fast Eva Green Supermix (Bio-Rad, USA), the amplification was carried out in Bio-Rad iCycler iQ5 RT-qPCR System. The temperature cycle of two-step RT-qPCR was as follows: pre-denatured at 95°C for 30 s; 39 cycles of denatured at 95°C for 5 s, annealed

and elongated at 56°C for 30 s. The statistical significance was detected by IBM-SPSS software.

Results

Transcriptomes: After quality filtration 32,836,885 and 27,597,990 clean reads were obtained from the RNA-seq data of *A. roxburghii* and *A. formosanus*, respectively, and assembled into unique transcripts. The longest, the total and the average length of the assembled transcripts were 16,083, 55,301,382, and 1,311 nt for *A. roxburghii*, and 15,675, 62,951, 915, and 986 nt for *A. formosanus*, respectively. Unigene from *A. roxburghii* and *A. formosanus* were annotated in the KGO database and classified into three broad categories: cellular components, biological processes, and molecular functions (Fig. 2A and 2B). The most unigene were classified as "general function prediction only" in both the *A. roxburghii* and *A. formosanus*. The putative protein of one of the assembled transcripts was annotated as *FPS* in *Dendrobium huoshanense* (GenBank accession number: KF891313.1), which belonged to another genus (*Dendrobium*) of the same family (*Orchidaceae*) with the genus *Anoectochilus*.

Open reading frames: With the primers designed based on the above information, a fragment of more than 1000 bp was amplified from the cDNA samples of *A. roxburghii* and *A. formosanus*, respectively (Fig. 3). The result of sequencing and alignment showed that they shared high similarity (99.6%) each other with only four bases different, and high homology (88.8% and 88.7%, respectively) with the ORFs of the *FPS* genes of *D. huoshanense* (Fig. 4).

Putative proteins: The putative proteins of the two amplified fragments were perfectly identical (100%) with each other, and shared high homology (87.6%) and the same conserved domains with the putative *FPS* protein of *D. huoshanense*. The four different bases between *A. roxburghii* and *A. formosanus* encoded the same amino acids (Fig. 5). The two putative proteins contained 348 amino acids with molecular weight 40.4 kDa, isoelectric point pI 5.23, and grand average of hydropathicity (GRAVY) -0.299. Their predicted secondary structure contained 35.9% α -helices, 20.4% extended strands and 43.7% random coils. All these properties were similar to those (molecular weight 40.4 kDa, pI 4.93, GRAVY -0.288, 36.2% α -helices, 20.1% extended strands and 43.7% random coils) of the putative *FPS* protein of *D. huoshanense*. Their three-dimensional structural model contained all the α -helices, extended strands and random coils of the *D. huoshanense* *FPS* (Fig. 6).

Functional domains: From the putative proteins of the two amplified fragments, no signal peptide was predicted by software SignalP 4.1 and TMHMM. Their subcellular localization was predicted to be cytoplasm with probabilities of 85.7% (Table 1). Seven conserved domains and two aspartate-rich motifs [DDXX(X)D] were found (Fig. 4).

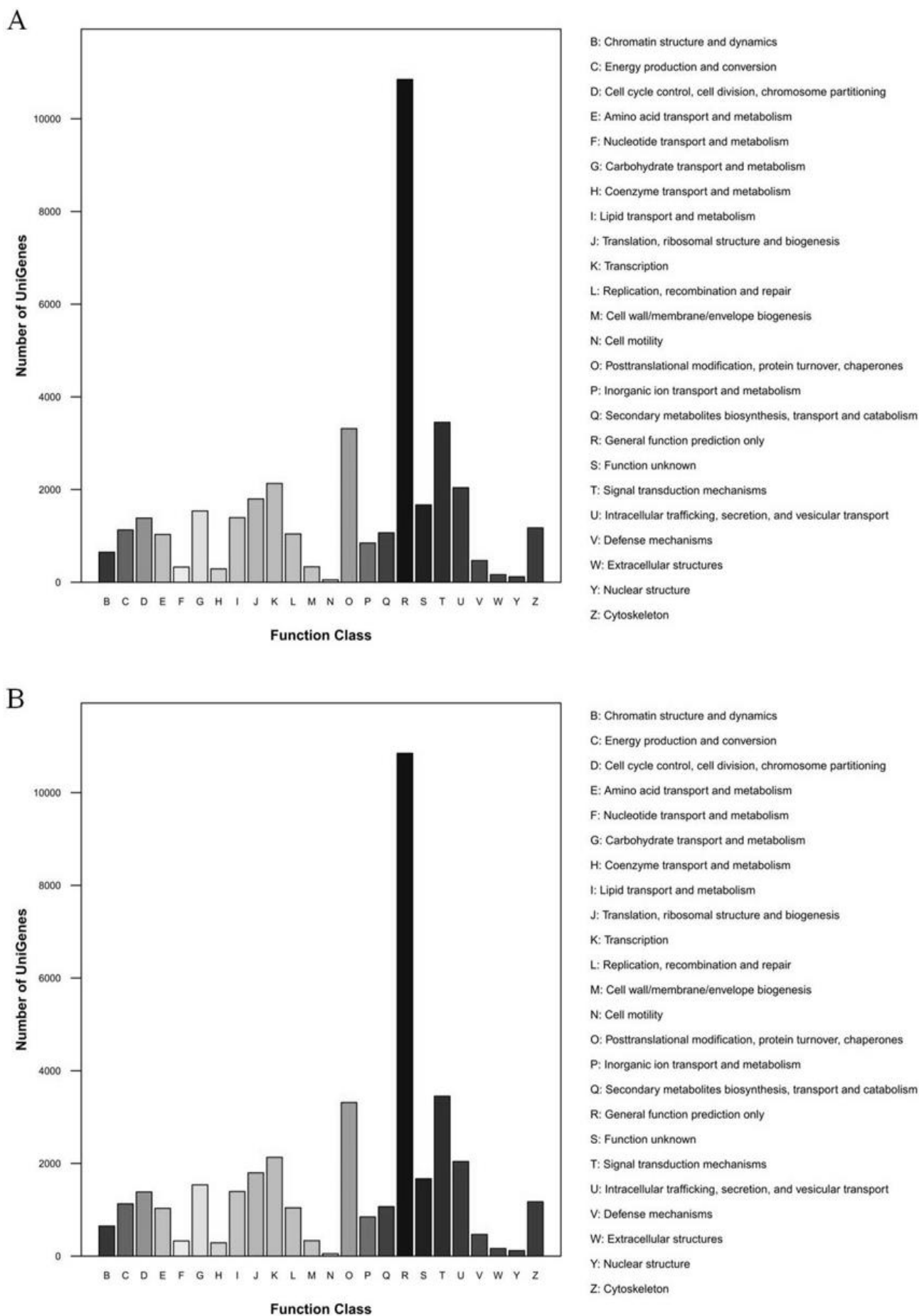


Fig. 2. Functional classification Unigene sequences of *A. formosanus* and *A. roxburghii* annotated against KOG. A: *A. formosanus*; B: *A. roxburghii*.

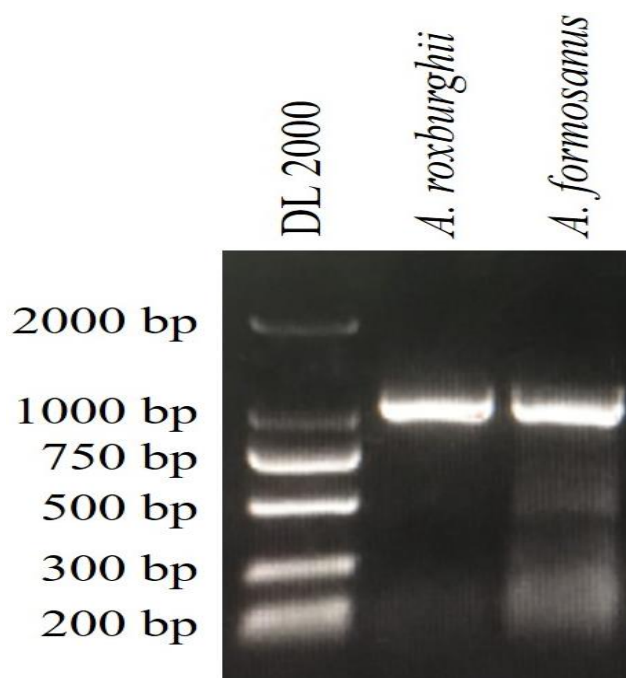


Fig. 3. The amplified fragments of the ORFs of the *FPS* genes from *A. roxburghii* and *A. formosanus*.

Phylogenetic relationship: Phylogenetic analysis showed that the putative proteins of the two amplified fragments were clustered into the same group with the deposited functional *FPS* proteins of other three species of family *Orchidaceae* (*Dendrobium huoshanense*, *Phalaenopsis equestris*, and *Cymbidium goeringii*) (Fig. 7). They should belong to the plant *FPS* super-family. The sum of branch length of the phylogenetic tree was 1.27857130.

According to the above results, the sequences of the two amplified fragments were identified as the ORFs of the *FPS* genes of *A. roxburghii* and *A. formosanus*, and registered at GenBank with accession numbers MH104945 and MH104946, respectively.

Subcellular localization: The green fluorescence protein was detected both in the cytoplasm and nucleus of the inner epidermis of onion transformed by the control vector pC2300–35S–*eGFP* and the expression vector pC2300–35S–*FPS*–*eGFP* (Fig. 8). This result confirmed the bioinformatics prediction for cytoplasm and nucleus localization of the *FPS* protein.

Relative expression level: Both in *A. roxburghii* and *A. formosanus*, the expression of the *FPS* genes was detectable from leaf, root, and stem, although their relative expression levels were significantly higher in root and stem (Fig. 9). In response to high salt treatment, the expression of the *FPS* gene was down regulated significantly in *A. roxburghii* and reached its valley at 8 h. In contrast, it kept constant in *A. formosanus* until a significant peak at the 24 h of the treatment (Fig. 10). Under the illumination of 650 nm red light and 253.7 nm UV, the overall trend of the expression of the *FPS* genes was down regulated, and reached its minimum at 4 h, although there was a peak value at the beginning (0.5 to 1 h of red light) (Figs. 11 and 12). However, the down

regulated range in *A. roxburghii* was narrower than that in *A. formosanus* under the illumination of 650 nm red light (Fig. 11).

Discussion

Seven conserved domains and two aspartate-rich motifs were found from *A. roxburghii* and *A. formosanus*, that were necessary for substrate binding and catalytic activity typical of other identified *FPS*s (Fig. 4; Ferriols *et al.*, 2015; Lan *et al.*, 2013; Su *et al.*, 2015). The high homology of the ORFs and putative protein sequences of *A. roxburghii* and *A. formosanus* with the deposited functional *FPS* proteins of *Dendrobium huoshanense* as well as other two species of family *Orchidaceae* (*Phalaenopsis equestris* and *Cymbidium goeringii*) indicated the high conservatism of the *FPS* genes and their importance in the revolution of *Orchidaceae* plants (Figs. 4, 5, 6 and 7). Many reports indicated their critical function in secondary metabolism of these plants (Liao *et al.*, 2006; Thabet *et al.*, 2011).

In several other plants, the *FPS* protein has been studied in subcellular localization (Thabet *et al.*, 2011; Krisans *et al.*, 1994; Sanmiya *et al.*, 1999). In the present study, the subcellular localization of the *FPS* protein was investigated in chloroplast-free epidermal cells of onion transformed by the in-frame fusion gene *FPS*–*eGFP*. The green fluorescent signal was detected in the cytoplasm and nucleus (Fig. 8).

In different plants, the expression of the *FPS* genes showed organic specificity, and the expression level was correlated to their accumulation of isoprenoidderivants (Gupta *et al.*, 2011; Lan *et al.*, 2013; Wang *et al.*, 2004; Xiang *et al.*, 2010; Yin *et al.*, 2011). In the present study, this kind of organic specificity was not very obvious (Fig. 9), but consistent with the general biosynthesis of terpenoids in all organs of *A. roxburghii* and *A. formosanus* (Chappell, 1995; Falcone Ferreyra *et al.*, 2012; Kim *et al.*, 2010; Szkopinska & Plochocka, 2005). However, the differential expression of the *FPS* genes in response to high salt treatment implies the different tolerance of the activities of *FPS* and terpenoid biosynthesis between these two species (Fig. 10). The constant and even upregulated response in *A. formosanus* indicated the higher tolerance of this species to saline stress than *A. roxburghii*, in which the expression of the *FPS* gene was downregulated in response to high salt treatment. The narrower range of downregulated expression of the *FPS* gene in *A. roxburghii* under the illumination of red light implies its higher suitability of terpenoid biosynthesis to shade environment of under forest than *A. formosanus* (Fig. 11), because the red light is less filtered by the upper vegetative canopy (Shao *et al.*, 2017). The gene expression response varies with type of abiotic stress (Mufti *et al.*, 2015; Nakashima *et al.*, 2000; Narusaka *et al.*, 1999; Narusaka *et al.*, 2001; Narusaka *et al.*, 2003; Shinwari *et al.*, 1998a,b). Therefore, we suggest that the cultivation of *A. formosanus* is probably more suitable for saline areas than *A. roxburghii*, and the latter is probably more suitable for cultivation under forest than the former.

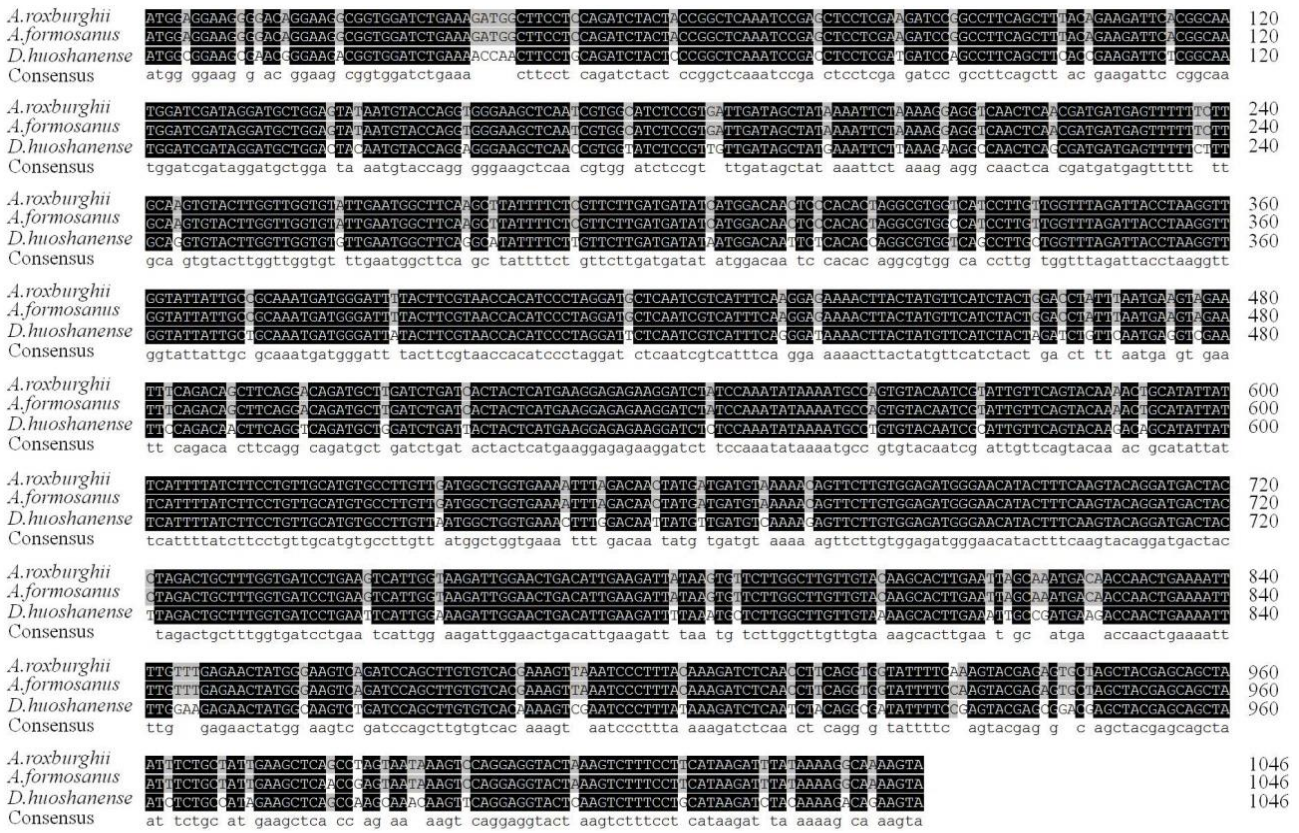


Fig.4. Multiple alignment of the ORFs of the FPS genes among *A. roxburghii*, *A. formosanus* and *D. huoshanense*. Identical and conserved bases are denoted by black (100%), gray (66.6%) and white (0%) backgrounds, respectively.

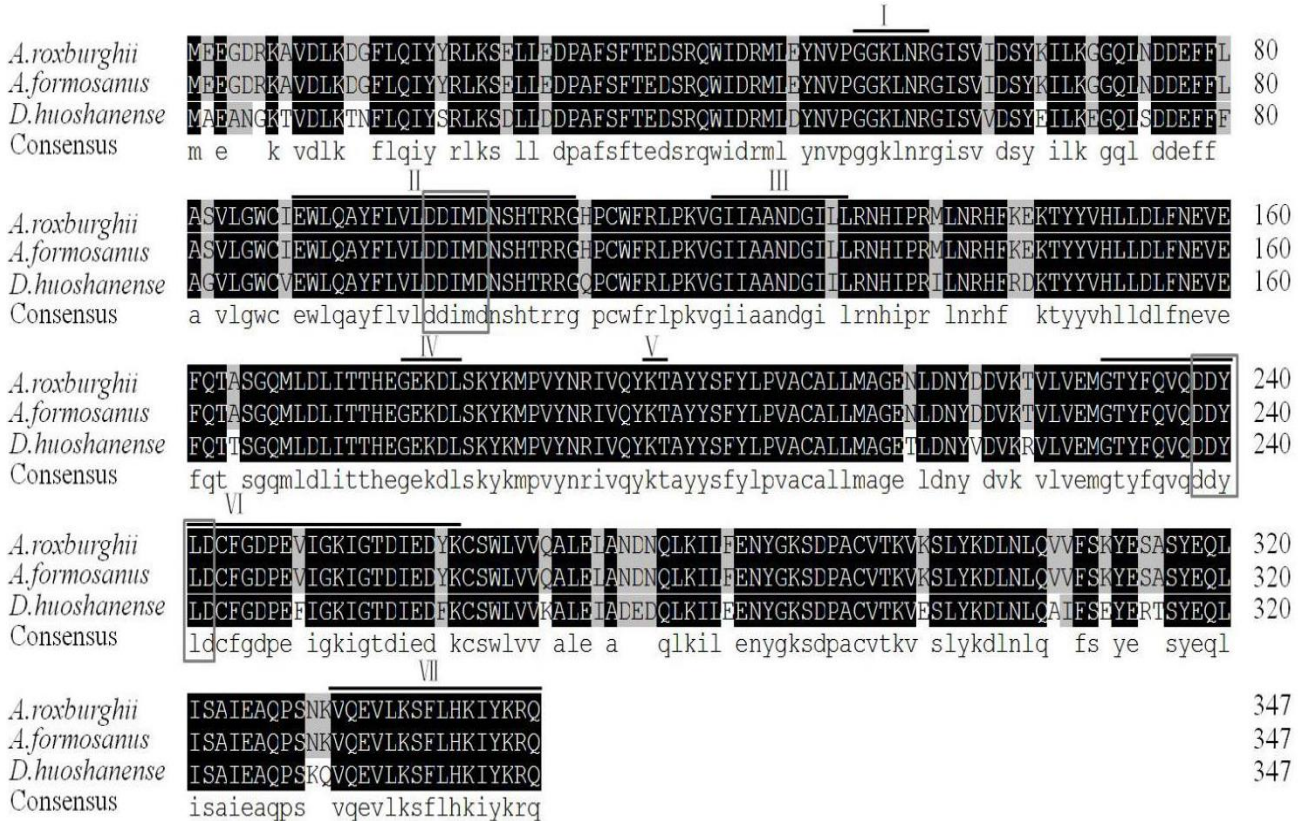


Fig. 5. Alignment of the putative proteins of the FPS genes among *A. roxburghii*, *A. formosanus* and *D. huoshanense*. Identical and conserved amino acid residues are denoted by black (100%), gray (66.6%) and white (0%) backgrounds, respectively. The seven conserved domains of prenyltransferases are marked with overlines and numbered from I to VII. Two highly conserved aspartate-rich motifs [DDXX(X)D] are present in the domains II and VI.

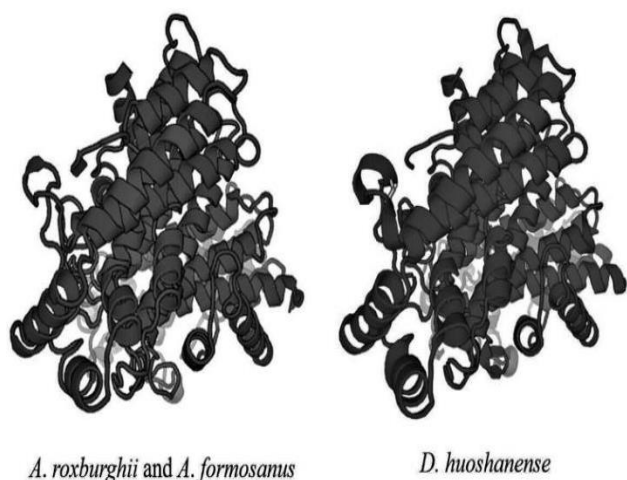


Fig.6. Predicted three-dimensional models of the putative proteins of the FPS genes between *A. roxburghii*, *A. formosanus* and *Dendrobium huoshanense*.

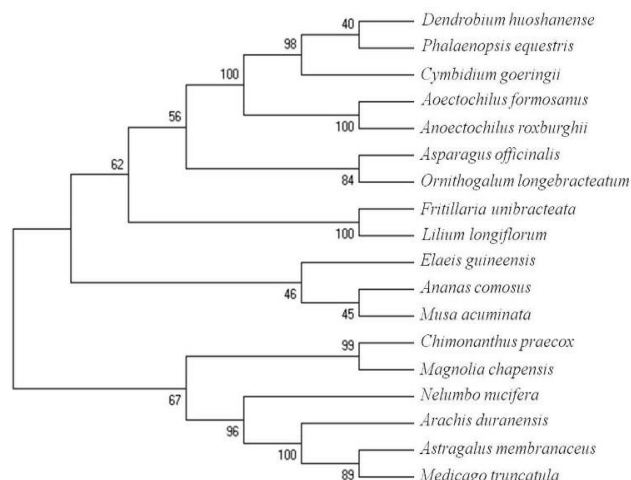


Fig.7. Phylogenetic tree among the putative proteins of *A. roxburghii*, *A. formosanus* and deposited functional FPS proteins of other plants.

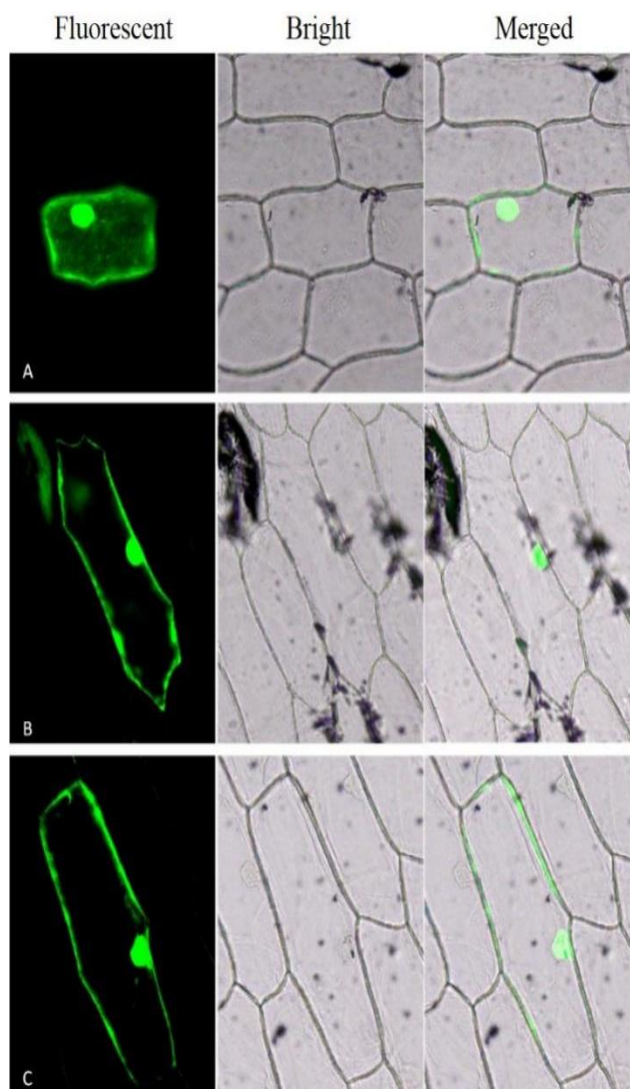


Fig. 8. Subcellular localization of FPS protein. eGFP and FPS-eGFP fusion gene were driven under the control of the CaMV 35S promoter. A Epidermal cells of onion transformed by pC2300-35S-eGFP. B Epidermal cells of onion transformed by pC2300-35S-FPS-eGFP from *A. formosanus*. C Epidermal cells of onion transformed by pC2300-35S-FPS-eGFP from *A. roxburghii*.

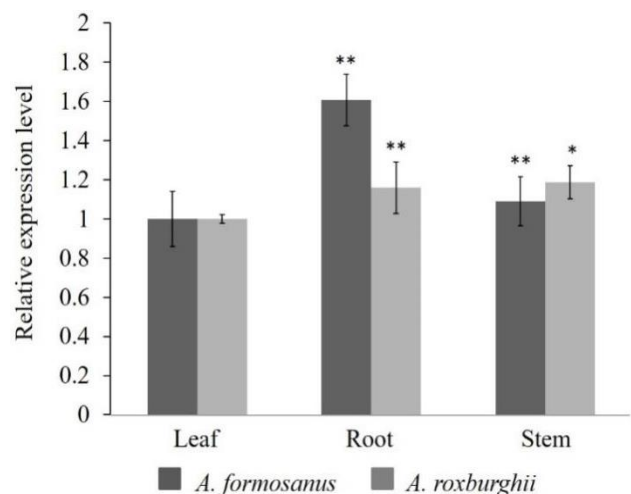


Fig. 9. Relative expression level of the FPS genes in different organs of *A. roxburghii* and *A. formosanus*. The asterisk (*) and double asterisk (**) stand for significance with the control at 0.05 and 0.01 levels, respectively.

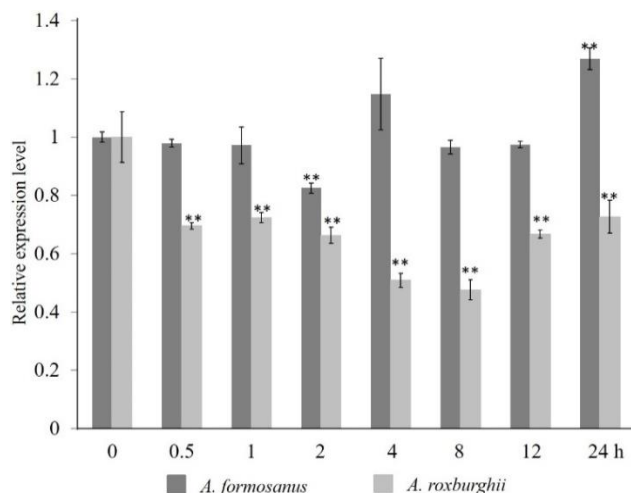


Fig. 10. Relative expression level of the FPS genes in response to high salt treatment in *A. roxburghii* and *A. formosanus*. The asterisk (*) and double asterisk (**) stand for significance with the control at 0.05 and 0.01 levels, respectively.

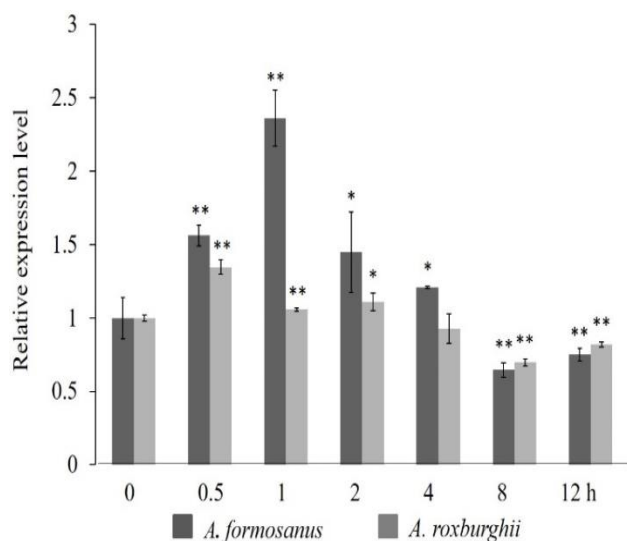


Fig. 11. Relative expression level of the *FPS* genes under the illumination of 650 nm red light in *A. roxburghii* and *A. formosanus*. The asterisk (*) and double asterisk (**) stand for significance with the control at 0.05 and 0.01 levels, respectively.

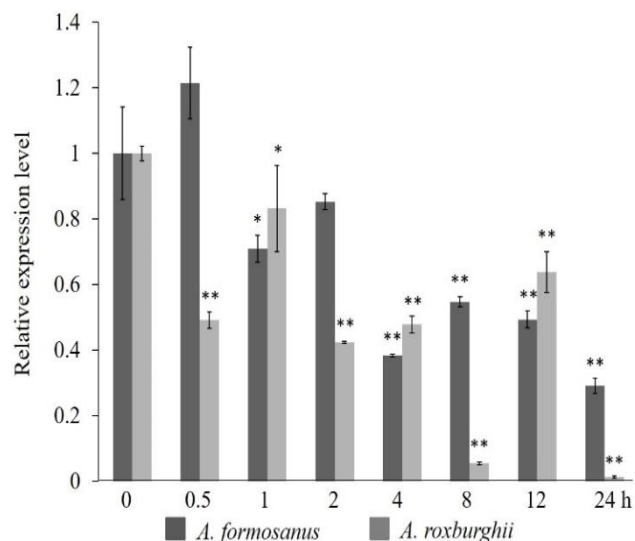


Fig. 12. Relative expression level of the *FPS* genes under the illumination of 253.7 nm UV in *A. roxburghii* and *A. formosanus*. The asterisk (*) and double asterisk (**) stand for significance with the control at 0.05 and 0.01 levels, respectively.

Table 1. Prediction of subcellular localization of the putative FPS proteins.

	<i>A. roxburghii</i>	<i>A. formosanus</i>	<i>D. huoshanense</i>	<i>C. goeringii</i>
<i>k</i> used for <i>kNN</i>	14	14	14	14
Cytoplasm	12	12	10	11
Nucleus	1	1	2	2
Plasmolemma	1	1		
Chloroplast			1	
Extra chrotrnasoma				1
Cytoskeleton			1	

Note: k-nearest neighbors algorithm (kNN) is a non-parametric method used for classification and regression (Hwang *et al.*, 1998). In total, 14 nearest neighborpoints were obtained and counted their classification in different organelles. The subcellular localization of the putative FPS proteins of *A. roxburghii* and *A. formosanus*, as well as two of their related species, were predicted to be in the cytoplasm with probabilities of 85.7% (13/14), 85.7% (13/14), 71.4% (13/14), and 78.6% (11/14), respectively

Conclusion

Based on transcriptomic analysis, the open reading frame sequences of the *FPS* genes were obtained from *A. roxburghii* and *A. formosanus*. After bioinformatics analysis, high homology of the FPS proteins and conserved domains was found in their orthologs in related species. The FPS-eGFP fusion protein was specifically distributed in the cytoplasm and nucleus. Meanwhile, the relative expressions of the *FPS* genes were significantly higher in root and stem, and responded to three different inductions. *A. formosanus* has higher tolerance to salt stress, and *A. roxburghii* is more suitable for cultivation under shade environment under forest.

Acknowledgments

This work was supported by Education Scientific Fund for Young Teachers from Fujian Education Department (JA15470) and Medicinal Plants Development and Utilization Center of Fujian (ZD1601), China.

References

- Arena, C., T. Tsonev, D. Doneva, V.D. Micco, M. Michelozzi and C. Brunetti. 2016. The effect of light quality on growth, photosynthesis, leaf anatomy and volatile isoprenoids of a monoterpene-emitting herbaceous species (*Solanum lycopersicum* L.) and an isoprene-emitting tree (*Platanus orientalis* L.). *Environ. Exp. Bot.*, 130: 122-132.
- Chappell, J. 1995. Biochemistry and molecular biology of the isoprenoid biosynthetic pathway in plants. *Ann. Rev. Plant. Physiol. Plant. MolBiol.*, 46: 521-547.
- Cheng, K.T., Y.S. Wang, H.C. Chou, C.C. Chang, C.K. Lee and S.H. Juan. 2015. Kinsenoside-mediated lipolysis through an AMPK-dependent pathway in C3H10T1/2 adipocytes: Roles of AMPK and PPAR α in the lipolytic effect of kinsenoside. *Phytomedicine*, 22: 641-647.
- Cock, P.J.A., C.J. Fields, N. Goto, M.L. Heuer and P.M. Rice. 2010. The Sanger FASTQ file format for sequences with quality scores, and the Solexa/Illumina FASTQ variants. *Nucl. Acids. Res.*, 38(6): 1767-1771.
- Cui, S.C., J. Yu, X.H. Zhang, M.Z. Cheng, L.W. Yang and J.Y. Xu. 2013. Antihyperglycemic and antioxidant activity of water extract from *Anoectochilus roxburghii* in experimental diabetes. *Exp. Toxicol. Pathol.*, 65: 485-488.

- Du, X.M., N. Irino, N. Furusho, J. Hayashi and Y. Shoyama. 2008. Pharmacologically active compounds in the *Anoectochilus* and *Goodyera* species. *J. Nat. Med.*, 62: 132-148.
- Du, X.M., N.Y. Sun, N. Irino and Y. Shoyama. 2000. Glycosidic constituents from *In vitro* *Anoectochilus formosanus*. *Chem. Pharm. Bull.*, 48: 1803-1804.
- Du, X.M., N.Y. Sun, T. Tamura, A. Mohri, M. Sugiura and T. Yoshizawa. 2001. Higher yielding isolation of kinsenoside in *Anoectochilus* and its anti-hyperlipidosis effect. *Biol. Pharm. Bull.*, 24: 65-69.
- Falcone-Ferreyra, M.L., S.P. Rius and P. Casati. 2012. Flavonoids: biosynthesis, biological functions, and biotechnological applications. *Front. Plant. Sci.*, 3: 222.
- Feng, C., M. Chen, C.J. Xu, L. Bai, X.R. Yin and X. Li. 2012. Transcriptomic analysis of Chinese bayberry (*Myricarubra*) fruit development and ripening using RNA-Seq. *Bmc. Genomics*, 13: 19-33.
- Ferriols, V.M., R. Yaginuma and M. Adachi. 2015. Cloning and characterization of farnesyl pyrophosphate synthase from the highly branched isoprenoid producing diatom *Rhizosoleniasetigera*. *Sci. Rep.*, 5: 10246.
- Grabherr, M.G., B.J. Haas, M. Yassour, J.Z. Levin, D.A. Thompson and I. Amit. 2011. Full-length transcriptome assembly from RNA-Seq data without a reference genome. *Nat. Biotechnol.*, 29: 644-652.
- Gupta, P., N. Akhtar, S.K. Tewari, R.S. Sangwan and P.K. Trivedi. 2011. Differential expression of farnesyl diphosphate synthase gene from *Withanasomnifera*, in different chemotypes and in response to elicitors. *Plant. Growth. Regul.*, 65: 93-100.
- Han, M.H., X.W. Yang and Y.P. Jin. 2010. Novel triterpenoid acyl esters and alkaloids from *Anoectochilus roxburghii*. *Phytochem. Anal.*, 19: 438-443.
- Hoagland, D. and D.I. Arnon. 1950. The water-culture method for growing plants without soil. *Calif. Agric. Exp. Stn. Circ.*, 347: 357-359.
- Hsiao, H.B., C.C. Hsieh, J.B. Wu, H. Lin and W.C. Lin. 2016. Kinsenoside inhibits the inflammatory mediator release in a type-II collagen induced arthritis mouse model by regulating the T cells responses. *BMC. Complement. Altern. Med.*, 16: 1-12.
- Hsiao, H.B., J.B. Wu, H. Lin and W.C. Lin. 2011. Kinsenoside isolated from *Anoectochilus formosanus* suppresses LPS-stimulated inflammatory reactions in macrophages and endotoxin shock in mice. *Shock*, 35: 184-190.
- Huang, L., Y. Cao, H. Xu and G. Chen. 2015. Separation and purification of ergosterol and stigmaterol in *Anoectochilus roxburghii* (Wall) Lindl by high-speed counter-current chromatography. *J. Sep. Sci.*, 34: 385-392.
- Hwang, W.J. and K.W. Wen. 1998. Fast kNN classification algorithm based on partial distance search. *Electron. Lett.*, 34: 2062-2063.
- Kim, O.T., S.H. Kim and K. Ohyama. 2010. Upregulation of phytosterol and triterpene biosynthesis in *Centellaasiatica* hairy roots overexpressed ginseng farnesyl diphosphate synthase. *Plant. Cell. Rep.*, 29: 403-411.
- Kim, Y.K., Y.B. Kim, M.R. Uddin, S. Lee, S.U. Kim and U.P. Sang. 2014. Enhanced triterpene accumulation in *Panax ginseng* hairy roots overexpressing mevalonate-5-pyrophosphate decarboxylase and farnesyl pyrophosphate synthase. *Acs. Synthetic. Biology*, 3: 773-779.
- Krisans, S.K., J. Ericsson, P.A. Edwards and G.A. Keller. 1994. Farnesyl-diphosphate synthase is localized in peroxisomes. *J. Biol. Chem.*, 269: 14165-14169.
- Lan, J.B., R.C. Yu, Y.Y. Yu and Y.P. Fan. 2013. Molecular cloning and expression of *Hedychium coronarium*, farnesyl pyrophosphate synthase gene and its possible involvement in the biosynthesis of floral and wounding/herbivory induced leaf volatile sesquiterpenoids. *Gene.*, 518: 360-367.
- Lang, K.Y., X.Q. Chen and Y.B. Luo. 1999. Angiospermae, in: The Editorial Board of Flora of China. (Eds.), Flora of China (Volume XVII). Science Press Beijing, pp. 220-227.
- Li, L., Y.M. Li, Z.L. Liu, J.G. Zhang, Q. Liu and L.T. Yi. 2016. The renal protective effects of *Anoectochilus roxburghii* polysaccharose on diabetic mice induced by high-fat diet and streptozotocin. *J. Ethnopharmacol.*, 178: 58-65.
- Liao, Z.H., M. Chen, Y.F. Gong, Z.G. Li, K.J. Zuo and P. Wang. 2006. A new farnesyl diphosphate synthase gene from *Taxus media*, Rehder: cloning, characterization and functional complementation. *J. Integr. Plant. Biol.*, 48(6): 8.
- Liu, Q., A.M. Qiao and L.Y. Yi. 2016. Protection of kinsenoside against AGEs-induced endothelial dysfunction in human umbilical vein endothelial cells. *Life. Sci.*, 162: 102-107.
- Liu, Z.L., J.G. Zhang, Q. Liu, L.T. Yi, Y.M. Li and Y. Li. 2017. The vascular protective effects of *Anoectochilus roxburghii* polysaccharose under high glucose conditions. *J. Ethnopharmacol.*, 18: 192-199.
- Mufti, F.U.D., S. Aman, S. Banaras, Z. K. Shinwari and S. Shakeel. 2015. *Actin* gene identification from selected medicinal plants for their use as internal controls for gene expression studies. *Pak. J. Bot.*, 47: 629-635.
- Murashige, T. and F. Skoog. 1962. A revised medium for rapid growth and bio assays with tobacco tissue cultures. *Physiol. Plant.*, 15: 473-497.
- Nakashima, K., Z.K. Shinwari, S. Miura, Y. Sakuma, M. Seki, K. Yamaguchi-Shinozaki and K. Shinozaki. 2000. Structural organization, expression and promoter activity of an Arabidopsis gene family encoding DRE/CRT binding proteins involved in dehydration- and high salinity-responsive gene expression. *Plant Mol. Biol.*, 42: 657-665.
- Narusaka, Y., K. Nakashima, Z. K. Shinwari, K. Shinozaki and K. Shinozaki. 2001. Promoter analysis of DREB1 genes encoding transcription factors involved in cold responsive gene expression in Arabidopsis. *Plant. Cell. Physiol.*, 42: 94.
- Narusaka, Y., K. Nakashima; Z.K. Shinwari, Y. Sakuma, T. Furihata, H. Abe, M. Narusaka, K. Shinozaki and K.Y. Shinozaki. 2003. Interaction between two cis-acting elements, ABRE and DRE, in ABA-dependent expression of Arabidopsis rd29A gene in response to dehydration and high salinity stresses. *The Plant J.*, 34: 137-149.
- Narusaka, Y., Z.K. Shinwari, K. Nakashima, K. Yamaguchi-Shinozaki and K. Shinozaki. 1999. The roles of the two Cis-Acting Elements, DRE and ABRE in the dehydration, high salt and low temperature responsive expression of the Rd29a gene in *Arabidopsis thaliana*. *Plant. Cell. Physiol.*, 40: 91.
- Patel, R.K. and M. Jain. 2012. NGS-QC Toolkit: a toolkit for quality control of next generation sequencing data. *PLoS. One*, 7: e30619.
- Sanmiya, K., O. Ueno and M. Matsuoka. 1999. Localization of farnesyl diphosphate synthase in chloroplasts. *Plant. Cell. Physiol.*, 40: 348-354.
- Shao, L., G.J. Liang, N. Liu and H.Y. Liang. 2017. Studies on cultivation under forest of *Anoectochilus roxburghii* at low altitude in Zhaoqing, Guangdong Province, China, *J. Trop. Subtrop. Bot.*, 25: 546-553.
- Shiau, Y.J., A.P. Sagare and U.C. Chen. 2002. Conservation of *Anoectochilus formosanus* Hayata by artificial cross-pollination and *In vitro* culture of seeds. *Bot. Bull. Acad. Sin.*, 43: 123-130.
- Shinwari, Z.K., K. Nakashima, S. Miura, M. Kasuga, K.Y. Shinozaki and K. Shinozaki. 1998a. Identification of a gene family encoding Dehydration-Responsive Element (DRE) binding factors in *Arabidopsis thaliana* and analysis of its promoter. *Plant. Cell. Physiol.*, 39: 106.
- Shinwari, Z.K., K. Nakashima, S. Miura, M. Kasuga, M. Seki, K. Yamaguchi-Shinozaki and K. Shinozaki. 1998b. An Arabidopsis gene family encoding DRE Binding Protein involved in low temperature- responsive gene expression. *Biochem. Biophys. Res. Commun.*, 250: 161-170.

- Shyur, L.F., C.H. Chen, C.P. Lo, S.Y. Wang, P.L. Kang and S.J. Sun. 2004. Induction of apoptosis in MCF-7 human breast cancer cells by phytochemicals from *Anoectochilus formosanus*. *J. Biomed. Sci.*, 11: 928-939.
- Su, S.S., H.M. Zhang and X.Y. Liu. 2015. Cloning and characterization of a farnesyl pyrophosphate synthase from *Matricaria recutita* L. and its upregulation by methyl jasmonate. *Genet. Mol. Res.*, 14: 349-361.
- Szkopinska, A. and D. Plochocka. 2005. Farnesyl diphosphate synthase: regulation of product specificity. *Acta. Bio. Chim. Pol.*, 52: 45-55.
- Thabet, I., G. Guirimand, V. Courdavault, N. Papon, S. Godet and C. Dutilleul. 2011. The subcellular localization of periwinkle farnesyl diphosphate synthase provides insight into the role of peroxisome in isoprenoid biosynthesis. *J. Plant. Physiol.*, 168: 2110-2116.
- Wang, P., Z. Liao, L. Guo, W. Li, M. Chen and Y. Pi. 2004. Cloning and functional analysis of a cDNA encoding *Ginkgo bilobafarnesyl* diphosphate synthase. *Mol. Cell.*, 18: 150-156.
- Wu, J.B., W.L. Lin, C.C. Hsieh, H.Y. Ho, H.S. Tsay and W.C. Lin. 2007. The hepatoprotective activity of kinsenoside from *Anoectochilus formosanus*. *Phytother. Res.*, 21: 58-61.
- Xiang, L., K. Zhao and L. Chen. 2010. Molecular cloning and expression of *Chimonanthus praecox* farnesyl pyrophosphate synthase gene and its possible involvement in the biosynthesis of floral volatile sesquiterpenoids. *Plant. Physiol. Bio. Chem.*, 48: 845-850.
- Xiang, M., T. Liu, W. Tan, H. Ren, H. Li and J. Liu. 2016. Effects of kinsenoside, a potential immunosuppressive drug for autoimmune hepatitis, on dendritic cells/CD8⁺ T cells communication in mice. *Hepatology*, 64: 2135-2150.
- Xiao, K.Q., R.C. Lai, R.S. Lin, G.H. Wu, W.R. Zheng and D.F. Wu. 2014. Effects of different culture conditions on main chemical compositions of *Anoectochilus roxburghii*. *Zhong. Yao. Cai.*, 37: 553-556.
- Yang, L.C., C.C. Hsieh, T.J. Lu and W.C. Lin. 2014. Structurally characterized arabinogalactan from *Anoectochilus formosanus* as an immuno-modulator against CT26 colon cancer in BALB/c mice. *Phytomedicine*, 21: 647-655.
- Yang, L.C., W.C. Lin and T.J. Lu. 2012. Characterization and prebiotic activity of aqueous extract and indigestible polysaccharide from *Anoectochilus formosanus*. *J. Agric. Food Chem.*, 60: 8590-8599.
- Yang, Z., X. Zhang, L. Yang, Q. Pan, J. Li and Y. Wu. 2017. Protective effect of *Anoectochilus roxburghii* polysaccharide against CCl₄-induced oxidative liver damage in mice. *Int. J. Biol. Macromol.*, 96: 442-450.
- Ye, S., Q. Shao, M. Xu, S. Li, M. Wu and X. Tan. 2017. Effects of light quality on morphology, enzyme activities, and bioactive compound contents in *Anoectochilus roxburghii*. *Front. Plant. Sci.*, 8: 857.
- Yin, T., X. Cao, Q. Miao, C. Li, X. Chen and M. Zhou. 2011. Molecular cloning and functional analysis of an organ-specific expressing gene coding for farnesyl diphosphate synthase from *Michelia chapensis*. *Dandy. Acta. Physiol. Plant.*, 33: 137-144.
- Yu, H.Q., W.Q. Feng, F.A. Su, Y.Y. Zhang, J.T. Qu, B.L. Liu, F.Z. Lu, L. Yang, F.L. Fu and W.C. Li. 2018. Cloning and characterization of BES1/BZR1 transcription factor genes in maize. *Plant. Growth. Regul.*, 86: 235-249.
- Zeng, B., M. Su, Q. Chen, Q. Chang, W. Wang and H. Li. 2016. Antioxidant and hepatoprotective activities of polysaccharides from *Anoectochilus roxburghii*. *Carbohydr. Polym.*, 153: 391-398.
- Zeng, B., M. Su, Q. Chen, Q. Chang, W. Wang and H. Li. 2017. Protective effect of a polysaccharide from *Anoectochilus roxburghii* against carbon tetrachloride-induced acute liver injury in mice. *J. Ethnopharmacol.*, 200: 124-135.
- Zhang, F.S., Y.L. Lv, H.L. Dong and S. Guo. 2010. Analysis of genetic stability through intersimple sequence repeats molecular markers in micropropagated plantlets of *Anoectochilus formosanus* Hayata, a medicinal plant. *Biol. Pharm. Bull.*, 33: 384-388.
- Zhang, G., M. Zhao, C. Song, A. Luo, J. Bai and S. Guo. 2012. Characterization of reference genes for quantitative real-time PCR analysis in various tissues of *Anoectochilus roxburghii*. *Mol. Biol. Rep.*, 39: 5905-5912.
- Zhang, J.G., Q. Liu, Z.L. Liu, L. Li and L.T. Yi. 2015. Antihyperglycemic activity of *Anoectochilus roxburghii* polysaccharose in diabetic mice induced by high-fat diet and streptozotocin. *J. Ethnopharmacol.*, 164: 180-185.
- Zhang, Y.H., J.Y. Cai, H.L. Ruan and J. Wu. 2007. Antihyperglycemic activity of kinsenoside, a high yielding constituent from *Anoectochilus roxburghii* in *Streptozotocin* diabetic rats. *J. Ethnopharmacol.*, 114: 141-145.
- Zhao, Y.J., X. Chen, M. Zhang, P. Su, Y.J. Liu and Y.R. Tong. 2015. Molecular cloning and characterization of farnesyl pyrophosphate synthase from *Tripterygium wilfordii*. *PLoS. One*, 10: e0125415.

(Received for publication 23 October 2018)